# Possibilities and impossibilities of magnetic nanoparticle use in the control of infectious biofilms

Quan, Kecheng; Zhang, Zexin; Ren, Yijin ; Busscher, Henk; van der Mei, Henny C.; Peterson, Brandon W.

*Published in:*
Journal of Materials Science & Technology

*DOI:*
10.1016/j.jmst.2020.08.031



*Publication date:*
2021

Journal of Materials Science & Technology 69 (2021) 69–78

Contents lists available at ScienceDirect

Journal of Materials Science & Technology

journal homepage: www.jmst.org

Invited Review

# Possibilities and impossibilities of magnetic nanoparticle use in the control of infectious biofilms

Kecheng Quan[a,b], Zexin Zhang[a,*], Yijin Ren[c], Henk J. Busscher[b,*], Henny C. van der Mei[b,*], Brandon W. Peterson[b]

[a] College of Chemistry, Chemical Engineering and Materials Science, Soochow University, Suzhou, 215123, China
[b] University of Groningen and University Medical Center Groningen, Department of Biomedical Engineering, 9713 AV, Groningen, the Netherlands
[c] University of Groningen and University Medical Center Groningen, Department of Orthodontics, Hanzeplein 1, 9713 GZ, Groningen, the Netherlands

ARTICLE INFO

*Article history:*
Received 5 June 2020
Received in revised form 11 July 2020
Accepted 18 July 2020
Available online 9 August 2020

*Keywords:*
Magnetic nanoparticles
Magnetic targeting
Biofilm
Infection
Antimicrobials

ABSTRACT

Targeting of chemotherapeutics towards a tumor site by magnetic nanocarriers is considered promising in tumor-control. Magnetic nanoparticles are also considered for use in infection-control as a new means to prevent antimicrobial resistance from becoming the number one cause of death by the year 2050. To this end, magnetic nanoparticles can either be loaded with an antimicrobial for use as a delivery vehicle or modified to acquire intrinsic antimicrobial properties. Magnetic nanoparticles can also be used for the local generation of heat to kill infectious microorganisms. Although appealing for tumor- and infection-control, injection in the blood circulation may yield reticuloendothelial uptake and physical obstruction in organs that yield reduced targeting efficiency. This can be prevented with suitable surface modification. However, precise techniques to direct magnetic nanoparticles towards a target site are lacking. The problem of precise targeting is aggravated in infection-control due to the micrometer-size of infectious biofilms, as opposed to targeting of nanoparticles towards centimeter-sized tumors. This review aims to identify possibilities and impossibilities of magnetic targeting of nanoparticles for infection-control. We first review targeting techniques and the spatial resolution they can achieve as well as surface-chemical modifications of magnetic nanoparticles to enhance their targeting efficiency and antimicrobial efficacy. It is concluded that targeting problems encountered in tumor-control using magnetic nanoparticles, are neglected in most studies on their potential application in infection-control. Currently biofilm targeting by smart, self-adaptive and pH-responsive, antimicrobial nanocarriers for instance, seems easier to achieve than magnetic targeting. This leads to the conclusion that magnetic targeting of nanoparticles for the control of micrometer-sized infectious biofilms may be less promising than initially expected. However, using propulsion rather than precise targeting of magnetic nanoparticles in a magnetic field to traverse through infectious-biofilms can create artificial channels for enhanced antibiotic transport. This is identified as a more feasible, innovative application of magnetic nanoparticles in infection-control than precise targeting and distribution of magnetic nanoparticles over the depth of a biofilm.



**Contents**



* Corresponding authors.
*E-mail addresses:* zhangzx@suda.edu.cn (Z. Zhang), h.j.busscher@umcg.nl (H.J. Busscher), h.c.van.der.mei@umcg.nl (H.C. van der Mei).

https://doi.org/10.1016/j.jmst.2020.08.031
1005-0302/

## 1. Introduction

Over 80% of all human bacterial infections are caused by bacteria growing in a biofilm-mode of growth [1]. Biofilms are defined as communities of surface-adhering and surface-adapted bacteria that grow in a self-produced matrix of extracellular polymeric substances (EPS). EPS acts as a glue, holding biofilm inhabitants together, and at the same time constitutes a barrier to the penetration and accumulation of antimicrobials in an infectious biofilm. Therewith, the biofilm-mode of growth contributes to antimicrobial-resistance. Antimicrobial-resistance is hard to beat by current antimicrobials and the number of antimicrobial-resistant bacterial strains and species is growing fast. As a result, infections by antimicrobial-resistant bacteria are predicted to become the main cause of death in the year 2050 [2].

Chemists are working over-time to develop novel antimicrobials to prevent this prediction from becoming true and especially nanotechnology-based novel infection-control strategies appear promising [3]. Existing antimicrobials can be encapsulated in smart, self-targeting and pH-responsive nanocarriers to kill bacteria in infectious biofilms [4]. These nanocarriers can be equipped with "stealth" properties that make them "invisible" in the blood circulation at physiological pH (7.4), but have strong affinity to negatively-charged bacteria once they come into the acidic environment of a biofilm that transforms their surface charge from a neutral or negative charge to a positive one [5–7]. Many novel nano-antimicrobials generate reactive-oxygen species to which most bacterial strains and species still have no adequate defense [8]. Photothermal nanoparticles that can locally generate high amounts of heat to kill infectious biofilm inhabitants, constitute a new class of nano-antimicrobials with an entirely new, antimicrobial working mechanism [7]. Other strategies to treat biofilms are the inhibition of quorum sensing which is particularly an effective method to treat *Pseudomonas aeruginosa* related cystic fibrosis [9,10] or enzyme-induced dispersal of biofilm by degradation of the biofilm matrix [11,12].

Magnetically-targetable nanoparticles with or without antimicrobial modification, are also new in the field of bacterial infections. Magnetic nanoparticles have been initially studied in order to target chemotherapeutics to a tumor site and its imaging [13–15]. Targeting of magnetic nanoparticles towards a tumor site using an external magnetic field can enhance drug accumulation in the tumor [16,17], as confirmed using magnetic resonance imaging [18–21]. Nevertheless, despite the relatively large size of tumors, magnetic targeting is not trivial requiring sophisticated techniques and surface modification to prevent reticuloendothelial uptake or physical obstruction in the liver or other organs during nanoparticle transport through the blood circulation [22].

Clinically, the problems associated with tumor treatment bear similarity with the treatment of infection. Moreover, a tumor represents a self-encapsulated environment with low pH and hypoxic conditions, as also existing in a biofilm. These considerations have stimulated extensive exploration of magnetic nanoparticles as a novel strategy for bacterial infection-control. Here, we provide a critical review of the use of magnetically-targetable nanoparticles as a novel infection-control strategy with the aim of deriving better insight in the *possibilities* and *impossibilities* of magnetic nanoparticles for the control of micrometer-sized infectious biofilms (see Table 1). The small size of infectious biofilms as compared with centimeter-sized tumors [24] makes magnetic targeting to biofilms technically challenging. Therefore, we will first start with an overview of magnetic nanoparticles, magnetic-targeting techniques and antimicrobial modification of magnetic nanoparticles. Secondly, we will discuss the applications of magnetic nanoparticles and magnetic-targeting techniques towards infectious biofilms. Finally, we will summarize the perspectives of the use of magnetic nanoparticles for infection-control.

**Table 1**
Size of clinically occurring infectious biofilms, measured as their longest diameter or length [23].

| Biofilm demonstrated in | Approximate size (μm) |
|---|---|
| Lung infections | 4-100 |
| Chronic wounds | 35-200 |
| Soft tissue fillers | 5-25 |
| Otitis media | 4-80 |
| Implant associated | 5-500 |
| Catheter and shunt associated | 5-1000 |
| Chronic osteomyelitis | 5-50 |
| Chronic rhinosinusitis | 5-30 |
| Contact lenses | 50-100 |

## 2. Strategies to fabricate magnetic nanoparticles

Magnetic nanoparticles can be prepared from highly saturated magnetization materials such as transition metals like Fe, Co, Ni and metal oxides like $Fe_3O_4$, $\gamma$-$Fe_2O_3$, according to a number of different methods. Pure metals such as iron nanoparticles possess the highest magnetization (up to 218 emu $g^{-1}$) [25,26] but usually also possess high toxicity and are prone to oxidation [27,28]. Therefore, pure metal nanoparticles are not considered suitable for biomedical applications. More stable and biocompatible metal oxides such as superparamagnetic iron oxide nanoparticles are preferred despite their lower magnetization (mostly lower than 100 emu $g^{-1}$) [13,25,29]. Moreover, antimicrobial surface functionalization is relatively easy for metal oxides [30].

Iron-based magnetic nanoparticles are most common and can be prepared by a variety of methods, summarized in Table 2. The simplest method is co-precipitation [31]. Preparation of large amounts of magnetic nanoparticles by co-precipitation is relatively easy, but as a disadvantage, often yields a non-uniform size distribution. More uniform size distributions can be obtained by thermal decomposition [32,33]. However, thermal decomposition requires high reaction temperatures up to 365 °C and use of an organic phase [34]. Hydrothermal reaction avoids the use of organic phases and can be done in an aqueous phase, while maintaining the advantages of thermal decomposition, including preparation of large amounts and a well-controlled size distribution. As a disadvantage, the reaction requires temperatures up to 200 °C that can only be achieved in an aqueous phase under high pressure during time periods of 8

**Table 2**
Summary of methods to prepare magnetic iron oxide-based nanoparticles (MIONPs), together with their respective advantages and disadvantages perceived.

| Material | Schematic preparation method | (+) Advantages/ (-) Disadvantages | Refs. |
|---|---|---|---|
| $Fe_3O_4$, $\gamma$-$Fe_2O_3$ | Co-precipitation 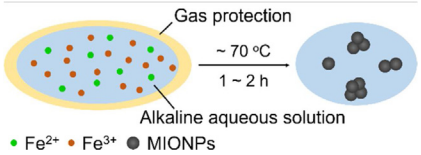  | (+) Facile preparation / (-) Large size distribution | [31] |
| $Fe_3O_4$, $\gamma$-$Fe_2O_3$, $MFe_2O_4$ (M = Fe, Co, Mn) | Thermal decomposition 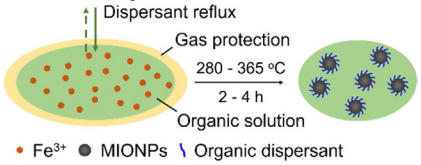  | (+) Narrow size distribution/ (-) High reaction temperature, use of an organic phase | [32–34] |
| Hollow/core-shell $Fe_3O_4$ | Hydrothermal synthesis 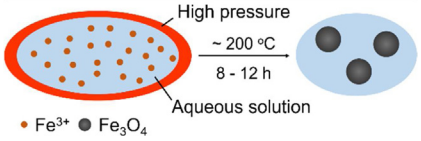  | (+) Well-controlled size distribution/ (-) High reaction temperature, high pressure and long reaction time | [35,36] |
| $Fe_3O_4$, $\gamma$-$Fe_2O_3$, $\alpha$-$Fe_2O_3$ | Sol-gel synthesis 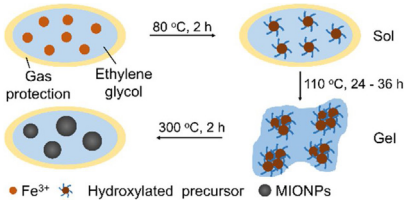  | (+) Well-controlled size and structure (-) Long reaction time | [37] |
| $Fe_3O_4$ | Electrochemical reaction 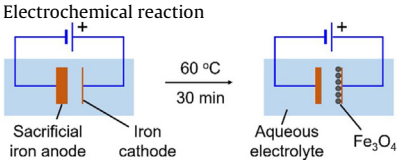  | (+) Facile size control/ (-) Poor reproducibility | [38] |
| $Fe_3O_4$, $Fe_2O_3$, FeO | Aerosol-vaporization 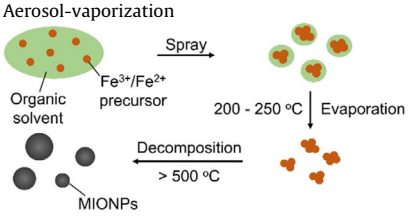  | (+) Large yields/ (-) High reaction temperature, large size distribution | [39,40] |
| $Fe_3O_4$ | Gas-phase deposition 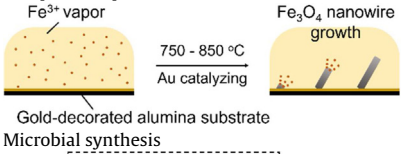  | (+) High structure control/ (-) High reaction temperature | [41] |
| $Fe_3O_4$, $Fe_3S_4$, $FeS_2$ | Microbial synthesis 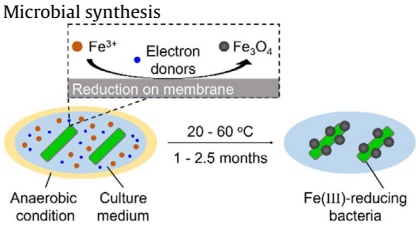  | (+) Large scale production, low temperature / (-) Long reaction time, large size distribution | [42,43] |

h or longer. Due to the high pressure necessary for hydrothermal reactions to prepare magnetic nanoparticles, special safety precautions are required [35,36]. Several other methods exist to prepare magnetic nanoparticles that are listed in Table 2, but these are less common in biomedical applications.

## 3. Techniques for targeting and imaging magnetic nanoparticles

Magnetic targeting is typically achieved by propulsion of magnetic nanoparticles using a magnetic field. Propulsion of magnetic

**Table 3**
Summary of targeting and imaging techniques of magnetic nanoparticles, together with their respective advantages and disadvantages. Spatial resolution was expressed in different units, depending on whether involving 2D, planar or 3D volumetric targeting.

| Targeting technique | Schematics | Spatialresolution | (+) Advantages/ (-) disadvantages | Refs. |
|---|---|---|---|---|
| Single-magnet | 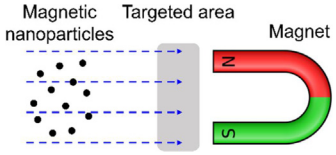  | 50-100 $mm^3$ | (+) Easy/ (-) One-directional and low spatial resolution | [47] |
| Multi- magnet | 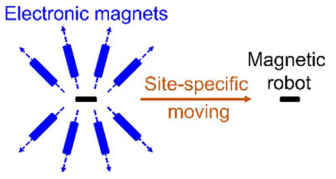  | 0.04-16 $mm^2$ | (+) High controllability/ (-) Insufficient observation in deep tissue | [51] |
| Magnetic particle imaging | 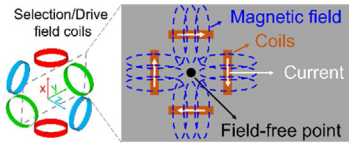  | 0.3-0.5 mm | (+) Real time imaging/ (-) Lack of transition to clinical application | [54] |

nanoparticles can be done at relatively low magnetic field strengths of less than 3 T, which causes no negative side-effects to human tissue [22,44]. Targeting, as opposed to simple propulsion, of magnetic nanoparticles towards a diseased site however, is not trivial and suffers from low spatial resolution and magnetic targeting efficiency, i.e. the percentage of magnetic nanoparticles that reach a target site. The easiest technique for magnetic targeting is to use a single-magnet (see Table 3) to attract magnetic nanoparticles to a target site [45,46]. Single-magnet targeting is frequently applied, either in laboratory or animal models [25,47–49]. However, single-magnet targeting is one-directional and critically depends on timing [50], which limits its targeting accuracy. A multi-magnet system consists of several electromagnets arranged in a spatial array to enable more accurate, multi-directional targeting. Often, multi-magnet targeting is done with electromagnets allowing to vary the magnetic field strength for precise targeting. As a result, millimeter resolution can be achieved in targeting of magnetic nanoparticles through the use of an eight magnet technique [51]. Jin et al. [22] used an eight magnet system for targeting of magnetic nanoparticles with millimeter resolution in a 2D experimental planar model with a high targeting efficiency of up to 89%. Yet, in real-life geometries, 3D millimeter resolution is more difficult to obtain than in experimental models, particularly in deep tissues [52].

For effective *in vivo* application of 3D targeting of magnetic nanoparticles, it is therefore desirable to combine targeting and real-time imaging of magnetic nanoparticles [53]. Magnetic Resonance Imaging (MRI) is clinically widely used for imaging. Theoretically MRI could also be used for targeting with a high spatial resolution, but in practice the magnetic field applied for targeting will interfere with the imaging process [53] and vice versa. In order to allow imaging without interfering with targeting, magnetic particle imaging (MPI) can be applied [54]. MPI is a tomographic imaging method initially designed to image magnetic tracers in the human body. MPI is based on application of an oscillating magnetic field in combination with a position-dependent, time-independent field. Since the magnetization curve of magnetic nanoparticles is non-linear, only nanoparticles positioned in the field-free point (see Table 3), show oscillating magnetization. Accordingly, magnetic nanoparticles can be imaged with a sub-millimeter resolution [54]. MPI however, is still under development. Taken together it must be concluded that high-efficiency, high-resolution targeting and imaging of magnetic nanoparticles is far from easy and may currently even be considered out of reach for micrometer-sized infectious biofilms.

## 4. Surface modification of magnetic nanoparticles to improve magnetic targeting efficiency

Although magnetic nanoparticles possess high biocompatibility even without surface modification [13], non-uniform size distribution and poor aqueous dispersibility affect the magnetic targeting efficiency *in vivo* [55]. Magnetic targeting efficiency of magnetic nanoparticles in absence of surface modification is relatively low *in vivo*, around 0.1% due to aggregation that increases reticuloendothelial uptake and yields physical obstruction in organs [16,56]. Surface modification of magnetic nanoparticles using poly(ethylene glycol) (PEG) or dextran can prevent aggregation by increasing the steric repulsion between nanoparticles and make the nanoparticles biologically invisible with reduced *in vitro* uptake in macrophages (Fig. 1(a)) [57] or *in vivo* obstruction in the liver or other organs (Fig. 1(b)) [56]. Modification of magnetic nanoparticles can also be done with inorganic materials such as silica, increasing their hydrophilicity to prevent aggregation and increase magnetic target efficiency [58]. Silica encapsulation also enables facile binding of other functional groups, but goes at the expense of magnetization of the nanoparticles [59].

## 5. Antimicrobial properties of magnetic nanoparticles

Magnetic nanoparticles can not only be modified to possess stealth properties aiding their magnetic targeting efficiency, but can also be antimicrobially modified, either implying their use as an antimicrobial delivery vehicle or equipping them with antimicrobial surface functionalities.

### 5.1. Magnetic nanoparticles as an antimicrobial delivery vehicle

Magnetic nanoparticles can aid antimicrobial transport in various ways. Encapsulation of iron oxide magnetic nanoparticles together with methicillin encapsulated in polymersomes [48] could be propelled into a methicillin-resistant *Staphylococcus epidermidis*

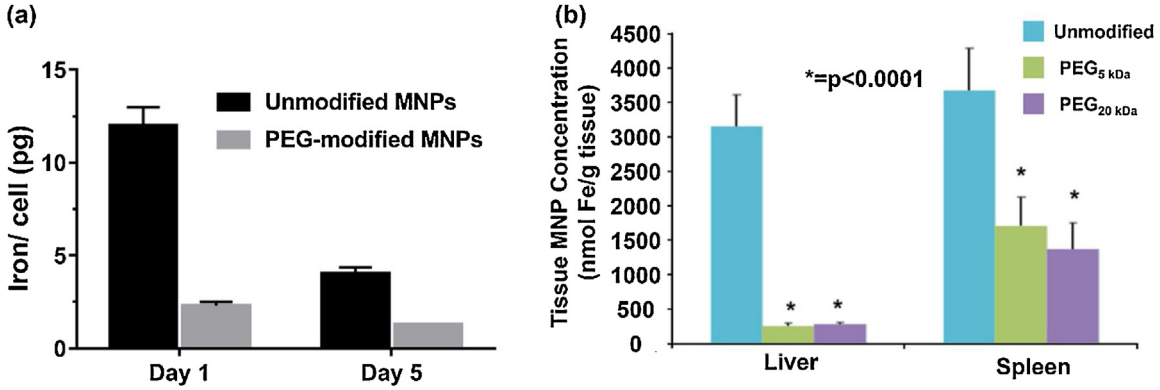


**Fig. 1.** Surface modification of magnetic nanoparticles to improve target efficiency. (a) *In vitro* uptake of unmodified superparamagnetic MNPs and PEG modified nanoparticles in mouse macrophages after one and five days of growth in presence of nanoparticles, data adapted from [43]. (With permission from Elsevier Ltd.). (b) Nanoparticle collection in the liver and spleen of rats 1 h post-administration of unmodified iron oxide MNPs and MNPs modified PEG of different molecular weight [42]. (With permission of Elsevier Ltd.).

biofilm under the influence of a single-magnet field to kill the majority of biofilm bacteria (Fig. 2(a)). In absence of encapsulation, Wang et al. [60] conjugated gentamicin to magnetic iron oxide nanoparticles for antibiotic delivery observing deep killing in *Staphylococcus aureus* biofilms, while Durmus and Webster [61] applied silver-conjugated superparamagnetic iron oxide nanoparticles to eradicate methicillin-resistant *S. aureus* biofilms (Fig. 2(b)). Magnetic iron oxide nanoparticles have also been modified to carry antimicrobial photodynamic agents into oral biofilms that create reactive oxygen species upon photo-irradiation [62].

Nearly all studies using magnetic propulsion to penetrate magnetic nanoparticles into a biofilm, assume homogeneous distribution of nanoparticles in biofilms (Fig. 2(c)), but this type of precise targeting is not trivial and requires extensive pilot studies before optimal magnetic field conditions are established. Distribution of gentamicin-loaded magnetic nanoparticles in an *S. aureus* biofilm depended critically upon magnetic field conditions [50]. Accumulation of nanoparticles near the surface of a biofilm or in its depth near to the substratum surface occurred due to overly short or long application times of a single-magnet field. This yielded a specific time duration for optimal distribution of gentamicin-loaded nanoparticles across the depth of a biofilm (Fig. 2(d)) and maximal killing of its inhabitants (Fig. 2(e)).

### 5.2. Magnetic nanoparticles as nano-antimicrobials

Iron oxide-based magnetic nanoparticles possess intrinsic antimicrobial properties, such as peroxidase-like enzyme mimetic activity enabling them to produce reactive oxygen species causing bacterial cell membrane damage [63] and therewith bacterial death [8,64]. Antimicrobial effects of carboxyl-grafted superparamagnetic iron oxide nanoparticles (SPIONs) magnetically targeted to staphylococcal biofilms were attributed to the generation of reactive oxygen species causing an oxidative stress [49,65]. Magnetically concentrated in a biofilm, carboxyl-grafted SPIONs caused an eight-fold higher percentage of dead staphylococci than gentamicin. Biofilm eradicating efficacy of SPIONs could be further improved in the presence of metabolic stimuli (i.e., fructose) due to the enhanced SPION uptake and antimicrobial sensitivity in a methicillin-resistant *S. aureus* (MRSA) biofilms [8]. SPION showed an 81% increase of killing efficacy in the presence of fructose and two orders of magnitude better killing than antibiotics.

## 6. Hyperthermia induced by magnetic nanoparticles as an antimicrobial strategy

Magnetic nanoparticles can locally generate heat upon exposure to an alternating current (AC) magnetic field. Heat can indiscriminately kill different bacterial strains with a low risk of inducing resistance. Magnetic hyperthermal treatment has therefore been considered promising for killing antibiotic-resistant bacterial infections after appropriate targeting [25,66]. However, without appropriate targeting, hyperthermia can be a double-edged sword that can kill not only pathogenic bacteria but also healthy tissue cells [67], which can limit its clinical applications.

Magnetic hypothermal treatment has so far been considered for eradication of *P. aeruginosa* biofilms (Fig. 3(a) and (b)) [68] and treatment of *S. aureus* infected wounds [69]. In addition, magnetic hypothermal treatment combined with antimicrobial use has shown synergistic effects towards eradication of infectious biofilms [66,70]. Magnetic hypothermia can also induce detachment of infectious bacteria from a biofilm (Fig. 3(c)) to allow subsequent easier killing of bacteria by antibiotics in their planktonic state [71]. Besides application of magnetic hypothermal treatment in infection-control, it is being considered to prevent bacterially-induced food spoilage caused by *Pseudomonas fluorescens* [72] and contamination of water by *Escherichia coli* [73].

## 7. Magnetic nanoparticles for disrupting the EPS matrix of an infectious biofilm

Apart from the intrinsic, peroxidase-like enzyme mimetic activity of iron oxide-based magnetic nanoparticles, their enzyme activity can also degrade the EPS that constitutes the matrix keeping biofilm inhabitants together [74]. In the presence of superparamagnetic iron oxide nanoparticles (SPIONs), $H_2O_2$ synergistically with SPIONs degraded the EPS matrix of *Streptococcus mutans* biofilm (Fig. 4(a)) and caused a more than 5-log reduction of cell viability that was absent for SPIONs or $H_2O_2$ only (Fig. 4(b)). However, the concentration of $H_2O_2$ used here was relatively high (1% v/v), which can be harmful to normal tissue [75] and may therefore limit clinical application.

The enzyme mimetic activity of iron oxide-based magnetic nanoparticles can also be used in a totally different way to affect the EPS matrix in a way that aids eradication of a biofilm. When magnetically propelled through a biofilm, these so-called Catalytic Antimicrobial microRobots (CARs) effectively broke down the EPS matrix of a biofilm (Fig. 5(a)) to completely remove biofilms

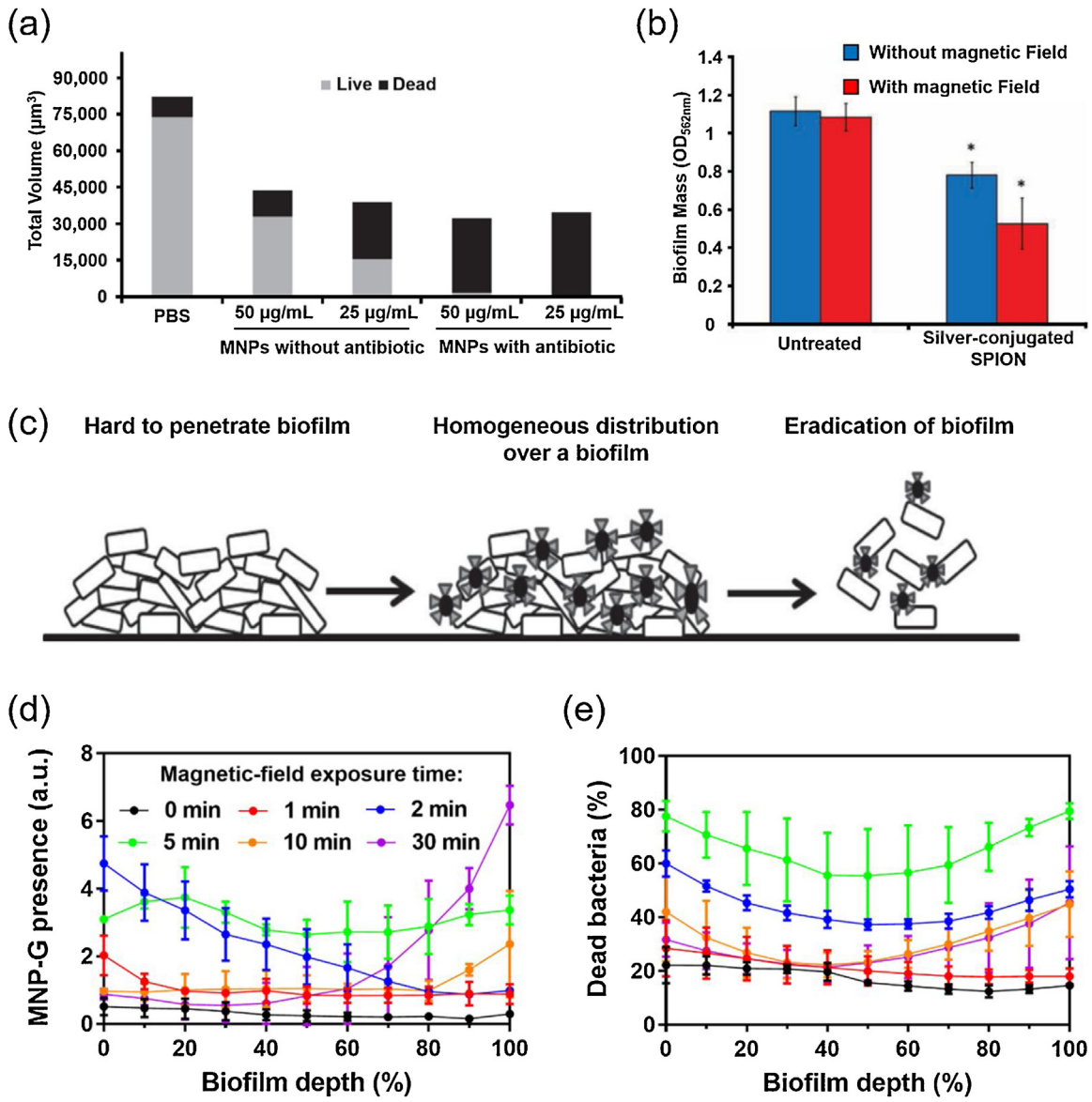


**Fig. 2.** Example of the use of antimicrobial-loaded magnetic nanoparticles for the control of infectious biofilms. (a) Total volume of methicillin-resistant *S. epidermidis* biofilms and fraction of live-to-dead bacteria upon 24 h exposure to polymersome-encapsulated iron oxide MNPs with and without methicillin after targeting in a single-magnet field, as quantified using confocal laser scanning microscopy [48]. (With permission from Elsevier Ltd.). (b) Mass of MRSA biofilms exposed to silver-conjugated superparamagnetic iron oxide nanoparticles (SPIONs) in absence and presence of a single-magnet field [61]. (With permission from Wiley). (c) Commonly assumed homogeneous distribution of MNP distribution across the depth of an infectious biofilms under an applied single-magnet field [61]. (With permission from Wiley). (d) Distribution of iron oxide MNPs with conjugated gentamicin across the depth of a *S. aureus* biofilm for different exposure times to a single-magnet field, showing homogeneous distribution for an exposure time of 5 min [50]. (With permission from American Chemical Society). (e) Similar as panel (d), showing maximal killing across the depth of a *S. aureus* biofilm for a magnet field exposure time of 5 min [50]. (With permission from American Chemical Society).

and biofilm debris from a surface, including dead bacteria and degraded EPS [76]. Magnetic iron oxide nanoparticles magnetically propelled through a biofilm have also been employed to create artificial water channels in *S. aureus* biofilms (Fig. 5(b)) to enhance antibiotic penetration and killing [77]. Digging of artificial channels by magnetically propelled nanoparticles in a staphylococcal biofilm increased the bacterial killing efficacy of gentamicin 4-6 fold. Importantly, this could be achieved by relatively rough, unprecise magnetic propulsion of magnetic nanoparticles in two perpendicular directions through a biofilm.

## 8. Summary and perspectives of the use of magnetic nanoparticles for infection-control

Major research efforts have been made to facilitate the use of magnetic nanoparticles for infection-control, most notably based on the possibility to direct magnetic nanoparticles to an infection-site using an applied magnetic field. Magnetic nanoparticles have three important intrinsic properties that make them suitable as an antimicrobial without further antimicrobial modification: (1) their ability to generate reactive oxygen species that can cause bacterial cell wall damage, (2) their photothermal properties through which they can locally generate heat to kill infectious bacteria, (3) their ability to disrupt the EPS matrix of a biofilm (see summary in Fig. 6). Apart from this, magnetic nanoparticles can be used as antimicrobial nanocarriers (Fig. 6). For *in vivo* use however, surface modification of magnetic nanoparticles is required to prevent their aggregation and therewith reticuloendothelial uptake and physical obstruction in organs.

The problems that arise in magnetic targeting of magnetic nanoparticles to micrometer-sized infection-sites are largely neglected in the current literature. Moreover, in general little atten-

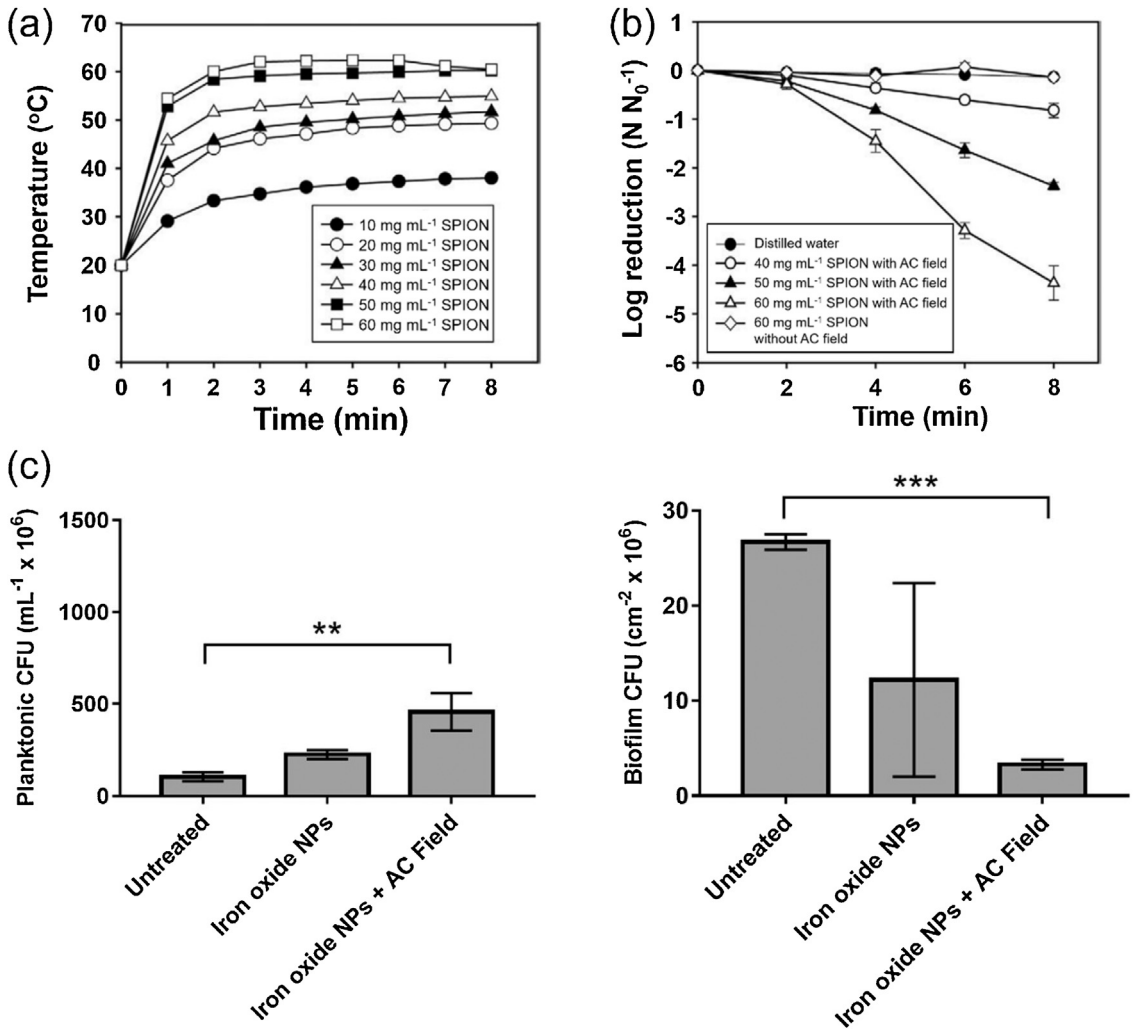


**Fig. 3.** Magnetic hypothermal treatment in infection-control. (a) Temperature of SPION suspensions with different SPION concentrations as a function of AC magnetic field application time. Suspension volume equals 0.15 mL, AC power and frequency 1.47 kW at 494 Hz and magnetic field strength amounts 3 kA $m^{-1}$, respectively [68]. (With permission from Elsevier Ltd.). (b) Log CFU reductions in *P. aeruginosa* biofilms exposed to SPION suspensions with different SPION concentrations as a function of AC magnetic field application time [68]. For details see panel (a). (With permission from Elsevier Ltd.). (c) Detachment of *P. aeruginosa* from biofilms exposed to iron oxide-based magnetic nanoparticles upon application of an AC magnetic field (left panel) and bacteria left behind in the biofilm (right panel) [71]. (With permission from Nature).

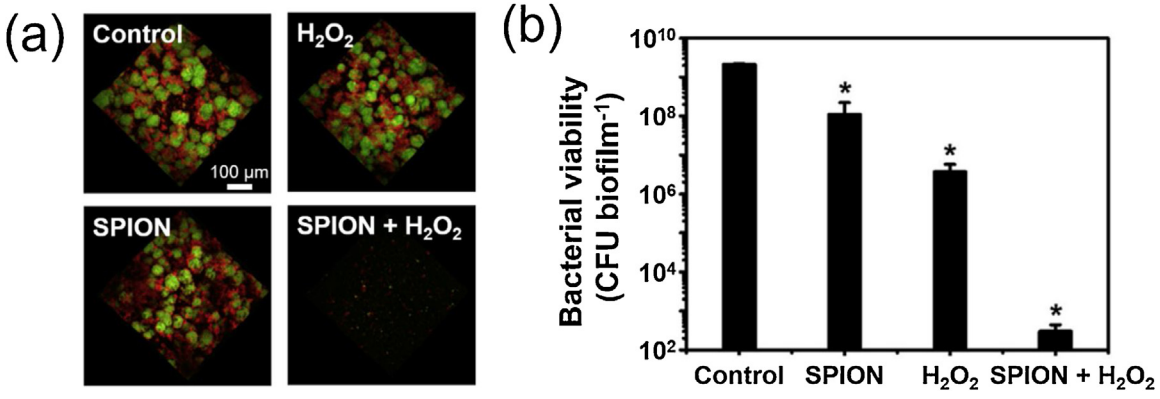


**Fig. 4.** Biofilm eradicating of magnetic nanoparticles by their peroxidase-like activity. (a) Confocal Laser Scanning Micrographs of *S. mutans* biofilm disruption after treatment with sodium acetate buffer (control), SPIONs followed by sodium acetate buffer exposure (SPION) or $H_2O_2$ exposure (SPION + $H_2O_2$), sodium acetate buffer followed by $H_2O_2$ exposure ($H_2O_2$). Green and red colours represent bacteria and EPS, respectively. (b) Bacterial cell viability in *S. mutans* biofilms according to panel (a) [74]. (With permission from Elsevier).

tion is given to describe the precise magnetic field conditions used. Yet, precise magnetic targeting, especially 3D targeting with micrometer resolution in deep tissues, is hard to obtain compared with chemical-targeting of nanoparticles. Smart, pH-responsive nanocarriers for instance, can target themselves to the low pH environment of an infectious biofilm *in vitro* [3]. Recently these smart

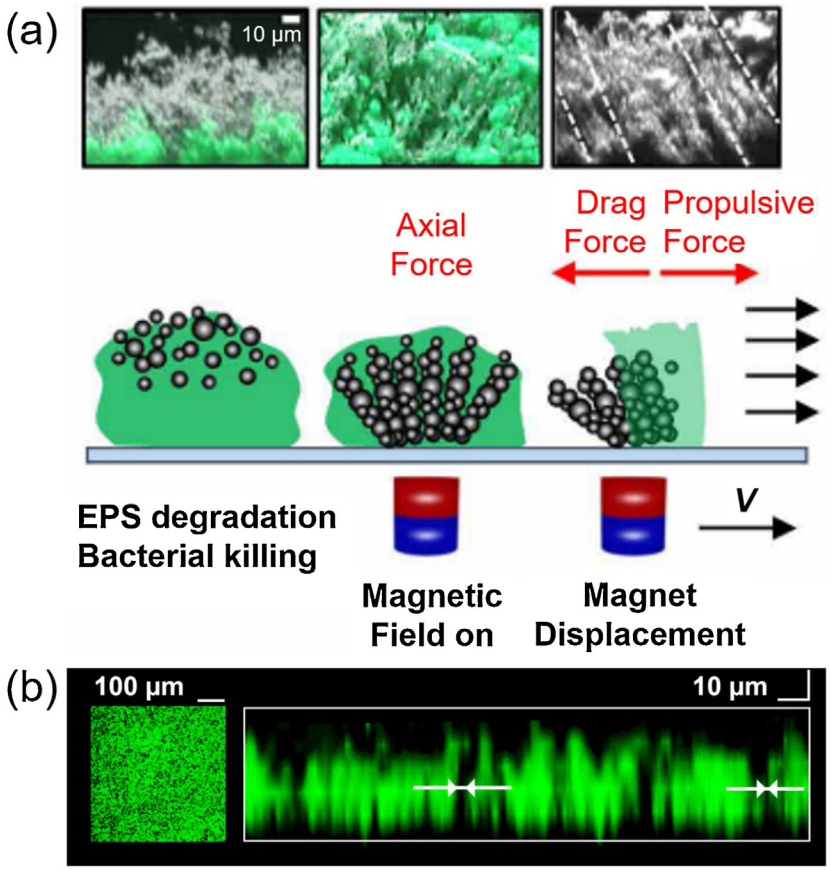


**Fig. 5.** Use of magnetically propelled nanoparticles for the control of infectious biofilms. (a) Cross-sectional view of *S. mutans* UA159 biofilms after having been traversed by catalytic, antimicrobial magnetic nanoparticles using a static magnetic field. Rod-like biofilm structures can be seen (white dashed lines) together with structural damage to the biofilm [76]. (With permission from AAAS). (b) Artificial channels created by magnetically-propelled MNPs to create artificial water channels in a biofilm, visible in the CLSM overlayer image of a green-fluorescent *S. aureus* as black holes, while indicate in the cross-sectional image by double-arrows [77]. (With permission from Wiley).

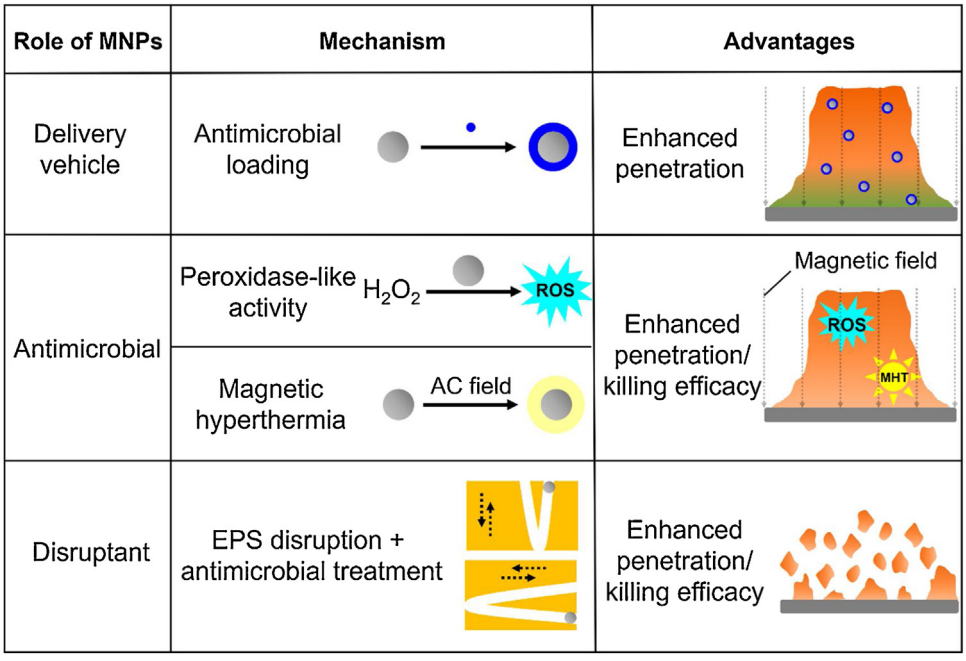


**Fig. 6.** Summary of advantages of magnetic nanoparticles as a novel nano-antimicrobial.

pH-responsive nanocarriers have been demonstrated *in vivo* to be able to find their own way through the blood circulation system towards a bacterial infection-site [78]. Since magnetic targeting of antimicrobial nanoparticles can currently not be achieved with the precision required to kill an infectious biofilm, this review yields the conclusion that clinical translation of the use of magnetic nanoparticles will remain out of reach unless precise, 3D magnetic targeting techniques becomes available.

However, alternative use of magnetic nanoparticles relying on magnetically propelling magnetic nanoparticles through a biofilm does not necessarily need targeting with the 3D resolution required to precisely target a biofilm and maintains a high concentration of magnetic nanoparticles inside the biofilm. Propelling magnetic nanoparticles through a biofilm has been shown to disrupt the biofilm matrix structure to allow better antibiotic penetration [77] and even cause complete removal of biofilm [76]. This type of use of magnetic nanoparticles possibly in combination with clinically used antibiotics (also see Fig. 6), is considered closer to clinical translation that requires precise targeting.

## Declaration of Competing Interest

The authors report no declarations of interest

## Acknowledgements

This work was financially supported by the National Key Research and Development Program of China (No. 2016YFC1100402), the National Natural Science Foundation of China (Nos. 11574222 and 21522404), and the University Medical Center Groningen (UMCG), The Netherlands.

## References

[1] D. Davies, Nat. Rev. Drug Discovery 2 (2003) 114–122.
[2] G. Humphreys, F. Fleck, Bull. W. H. O. 94 (2016) 638–639.
[3] Y. Liu, L. Shi, L. Su, H.C. van der Mei, P.C. Jutte, Y. Ren, H.J. Busscher, Chem. Soc. Rev. 48 (2019) 428–446.
[4] Y. Liu, H.J. Busscher, B. Zhao, Y. Li, Z. Zhang, H.C. van der Mei, Y. Ren, L. Shi, ACS Nano 10 (2016) 4779–4789.
[5] D. Hu, Y. Deng, F. Jia, Q. Jin, J. Ji, ACS Nano 14 (2020) 347–359.
[6] Y. Gao, J. Wang, M. Chai, X. Li, Y. Deng, Q. Jin, J. Ji, ACS Nano 14 (2020) 5686–5699.
[7] Y. Liu, H.C. van der Mei, B. Zhao, Y. Zhai, T. Cheng, Y. Li, Z. Zhang, H.J. Busscher, Y. Ren, L. Shi,Adv. Funct. Mater. 27 (2017), 1701974.
[8] N.G. Durmus, E.N. Taylor, K.M. Kummer, T.J. Webster, Adv. Mater. 25 (2013) 5706–5713.
[9] N. Singh, M. Romero, A. Travanut, P.F. Monteiro, E. Jordana-Lluch, K.R. Hardie, P. Williams, M.R. Alexander, C. Alexander, Biomater. Sci. 7 (2019) 4099–4111.
[10] N. Nafee, A. Husari, C.K. Maurer, C. Lu, C. De Rossi, A. Steinbach, R.W. Hartmann, C.M. Lehr, M. Schneider, J. Controlled Release 192 (2014) 131–140.
[11] J.J.T.M. Swartjes, T. Das, S. Sharifi, G. Subbiahdoss, P.K. Sharma, B.P. Krom, H.J. Busscher, H.C. van der Mei, Adv. Funct. Mater. 23 (2013) 2843–2849.
[12] P.J. Weldrick, M.J. Hardman, V.N. Paunov, ACS Appl. Mater. Interfaces 11 (2019) 43902–43919.
[13] A.K. Gupta, M. Gupta, Biomaterials 26 (2005) 3995–4021.
[14] K. Ulbrich, K. Holá, V. Šubr, A. Bakandritsos, J. Tuček, R. Zbořil, Chem. Rev. 116 (2016) 5338–5431.
[15] L.H. Reddy, J.L. Arias, J. Nicolas, P. Couvreur, Chem. Rev. 112 (2012) 5818–5878.
[16] B. Chertok, B.A. Moffat, A.E. David, F. Yu, C. Bergemann, B.D. Ross, V.C. Yang, Biomaterials 29 (2008) 487–496.
[17] A.J. Cole, A.E. David, J. Wang, C.J. Galbán, H.L. Hill, V.C. Yang, Biomaterials 32 (2011) 2183–2193.
[18] H. Han, Y. Hou, X. Chen, P. Zhang, M. Kang, Q. Jin, J. Ji, M. Gao, J. Am. Chem. Soc. 142 (2020) 4944–4954.
[19] X. Jiang, S. Zhang, F. Ren, L. Chen, J. Zeng, M. Zhu, Z. Cheng, M. Gao, Z. Li, ACS Nano 11 (2017) 5633–5645.
[20] J. Yu, Y. Ju, L. Zhao, X. Chu, W. Yang, Y. Tian, F. Sheng, J. Lin, F. Liu, Y. Dong, Y. Hou, ACS Nano 10 (2016) 159–169.
[21] Y. Guo, Y. Ran, Z. Wang, J. Cheng, Y. Cao, C. Yang, F. Liu, H. Ran,Biomaterials 219 (2019), 119370.
[22] Z. Jin, K.T. Nguyen, G. Go, B. Kang, H.K. Min, S.J. Kim, Y. Kim, H. Li, C.S. Kim, S. Lee, S. Park, K.P. Kim, K.M. Huh, J. Song, J.O. Park, E. Choi, Nano Lett. 19 (2019) 8550–8564.
[23] T. Bjarnsholt, M. Alhede, M. Alhede, S.R. Eickhardt-Sørensen, C. Moser, M. Kühl, P.Ø. Jensen, N. Høiby, Trends Microbiol. 21 (2013) 466–474.
[24] M.M. Tomayko, C.P. Reynolds, Cancer Chemother. Pharmacol. 24 (1989) 148–154.
[25] Y. Chao, G. Chen, C. Liang, J. Xu, Z. Dong, X. Han, C. Wang, Z. Liu, Nano Lett. 19 (2019) 4287–4296.
[26] L.M. Lacroix, N. Frey Huls, D. Ho, X. Sun, K. Cheng, S. Sun, Nano Lett. 11 (2011) 1641–1645.
[27] N. Tran, T.J. Webster, J. Mater. Chem. 20 (2010) 8760–8767.
[28] J.T. Nurmi, P.G. Tratnyek, V. Sarathy, D.R. Baer, J.E. Amonette, K. Pecher, C. Wang, J.C. Linehan, D.W. Matson, R.L. Penn, M.D. Driessen, Environ. Sci. Technol. 39 (2005) 1221–1230.
[29] A.E. Deatsch, B.A. Evans, J. Magn. Magn. Mater. 354 (2014) 163–172.
[30] M.M. El-Hammadi, J.L. Arias, Expert Opin. Ther. Pat. 25 (2015) 691–709.
[31] W. Wu, Q. He, C. Jiang, Nanoscale Res. Lett. 3 (2008) 397–415.
[32] S. Sun, H. Zeng, J. Am. Chem. Soc. 124 (2002) 8204–8205.
[33] S. Sun, H. Zeng, D.B. Robinson, S. Raoux, P.M. Rice, S.X. Wang, G. Li, J. Am. Chem. Soc. 126 (2004) 273–279.
[34] J. Park, K. An, Y. Hwang, J. Park, H. Noh, J. Kim, J. Park, N. Hwang, T. Hyeon, Nat. Mater. 3 (2004) 891–895.
[35] W. Cheng, K. Tang, Y. Qi, J. Sheng, Z. Liu, J. Mater. Chem. 20 (2010) 1799–1805.
[36] J. Liu, Z. Sun, Y. Deng, Y. Zou, C. Li, X. Guo, L. Xiong, Y. Gao, F. Li, D. Zhao, Angew. Chem. Int. Ed. 48 (2009) 5875–5879.
[37] G.M. Da Costa, E. De Grave, P.M.A. De Bakker, R.E. Vandenberghe, J. Solid State Chem. 113 (1994) 405–412.
[38] L. Cabrera, S. Gutierrez, N. Menendez, M.P. Morales, P. Herrasti, Electrochim. Acta 53 (2008) 3436–3441.
[39] T. González-Carreño, A. Misfsud, C.J. Serna, J.M. Palacios, Mater. Chem. Phys. 27 (1991) 287–296.
[40] T. González-Carreño, M.P. Morales, M. Gracia, C.J. Serna, Mater. Lett. 18 (1993) 151–155.
[41] S. Mathur, S. Barth, U. Werner, F. Hernandez-Ramirez, A. Romano-Rodriguez, Adv. Mater. 20 (2008) 1550–1554.
[42] J.W. Moon, C.J. Rawn, A.J. Rondinone, L.J. Love, Y. Roh, S.M. Everett, R.J. Lauf, T.J. Phelps, J. Ind. Microbiol. Biotechnol. 37 (2010) 1023–1031.
[43] K.B. Narayanan, N. Sakthivel, Adv. Colloid Interface Sci. 156 (2010) 1–13.
[44] X. Wang, C. Ho, Y. Tsatskis, J. Law, Z. Zhang, M. Zhu, C. Dai, F. Wang, M. Tan, S. Hopyan, H. McNeill, Y. Sun, Sci. Rob. 4 (2019) eaav6180.
[45] B. Chertok, A.E. David, V.C. Yang, Biomaterials 31 (2010) 6317–6324.
[46] A.S. Lübbe, C. Bergemann, H. Riess, F. Schriever, P. Reichardt, K. Possinger, M. Matthias, B. Dörken, F. Herrmann, R. Gürtler, P. Hohenberger, N. Haas, R. Sohr, B. Sander, A.J. Lemke, D. Ohlendorf, W. Huhnt, D. Huhn, Cancer Res. 56 (1996) 4686–4693.
[47] K. Lee, A.E. David, J. Zhang, M.C. Shin, V.C. Yang, J. Ind. Eng. Chem. 54 (2017) 389–397.
[48] B.M. Geilich, I. Gelfat, S. Sridhar, A.L. van de Ven, T.J. Webster, Biomaterials 119 (2017) 78–85.
[49] G. Subbiahdoss, S. Sharifi, D.W. Grijpma, S. Laurent, H.C. van der Mei, M. Mahmoudi, H.J. Busscher, Acta Biomater. 8 (2012) 2047–2055.
[50] K. Quan, Z. Zhang, Y. Ren, H.J. Busscher, H.C. van der Mei, B.W. Peterson, ACS Biomater. Sci. Eng. 6 (2020) 205–212.
[51] F. Ullrich, C. Bergeles, J. Pokki, O. Ergeneman, S. Erni, G. Chatzipirpiridis, S. Pané, C. Framme, B.J. Nelson, Invest. Ophthalmol. Visual Sci. 54 (2013) 2853–2863.
[52] B. Shapiro, S. Kulkarni, A. Nacev, A. Sarwar, D. Preciado, D.A. Depireux, Annu. Rev. Biomed. Eng. 16 (2014) 455–481.
[53] B. Shapiro, S. Kulkarni, A. Nacev, S. Muro, P.Y. Stepanov, I.N. Weinberg, Wiley Interdiscip. Rev. Nanomed. Nanobiotechnol. 7 (2015) 446–457.
[54] B. Gleich, J. Weizenecker, Nature 435 (2005) 1214–1217.
[55] Y.X.J. Wang, S.M. Hussain, G.P. Krestin, Eur. Radiol. 11 (2001) 2319–2331.
[56] A.J. Cole, A.E. David, J. Wang, C.J. Galbán, V.C. Yang, Biomaterials 32 (2011) 6291–6301.
[57] Y. Zhang, N. Kohler, M. Zhang, Biomaterials 23 (2002) 1553–1561.
[58] N. Zhu, H. Ji, P. Yu, J. Niu, M.U. Farooq, M.W. Akram, I.O. Udego, H. Li, X. Niu, Nanomaterials 8 (2018) 810.
[59] M. Abbas, B. Parvatheeswara Rao, M. Nazrul Islam, S.M. Naga, M. Takahashi, C. Kim, Ceram. Int. 40 (2014) 1379–1385.
[60] X. Wang, A. Deng, W. Cao, Q. Li, L. Wang, J. Zhou, B. Hu, X. Xing, J. Mater. Sci. 53 (2018) 6433–6449.
[61] N.G. Durmus, T.J. Webster, Adv. Healthcare Mater. 2 (2013) 165–171.
[62] X. Sun, L. Wang, C.D. Lynch, X. Sun, X. Li, M. Qi, C. Ma, C. Li, B. Dong, Y. Zhou, H.H.K. Xu, J. Dent. 81 (2019) 70–84.
[63] L. Gao, J. Zhuang, L. Nie, J. Zhang, Y. Zhang, N. Gu, T. Wang, J. Feng, D. Yang, S. Perrett, X. Yan, Nat. Nanotechnol. 2 (2007) 577–583.
[64] E.N. Taylor, K.M. Kummer, N.G. Durmus, K. Leuba, K.M. Tarquinio, T.J. Webster, Small 8 (2012) 3016–3027.
[65] K.D. Leuba, N.G. Durmus, E.N. Taylor, T.J. Webster, Int. J. Nanomed. 8 (2013) 731–736.
[66] E.C. Abenojar, S. Wickramasinghe, M. Ju, S. Uppaluri, A. Klika, J. George, W. Barsoum, S.J. Frangiamore, C.A. Higuera-Rueda, A.C.S. Samia, ACS Infect. Dis. 4 (2018) 1246–1256.
[67] X. Ren, R. Gao, H.C. van der Mei, Y. Ren, B.W. Peterson, H.J. Busscher, ACS Appl. Mater. Interfaces (2020), http://dx.doi.org/10.1021/acsami.0c08592.
[68] H. Park, H.J. Park, J.A. Kim, S.H. Lee, J.H. Kim, J. Yoon, T.H. Park, J. Microbiol, Methods 84 (2011) 41–45.

[69] M.H. Kim, I. Yamayoshi, S. Mathew, H. Lin, J. Nayfach, S.I. Simon, Ann. Biomed. Eng. 41 (2013) 598–609.
[70] C.H. Fang, P.I. Tsai, S.W. Huang, J.S. Sun, J.Z.C. Chang, H.H. Shen, S.Y. Chen, F.H. Lin, L.T. Hsu, Y.C. Chen, BMC Infect. Dis. 17 (2017) 516.
[71] T.K. Nguyen, H.T.T. Duong, R. Selvanayagam, C. Boyer, N. Barraud, Sci. Rep. 5 (2015) 18385.
[72] D. Rodrigues, M. Bañobre-López, B. Espiña, J. Rivas, J. Azeredo, Biofouling 29 (2013) 1225–1232.
[73] S.F. Situ, J. Cao, C. Chen, E.C. Abenojar, J.M. Maia, A.C.S. Samia, Macromol. Mater. Eng. 31 (2016) 1525–1536.
[74] L. Gao, Y. Liu, D. Kim, Y. Li, G. Hwang, P.C. Naha, D.P. Cormode, H. Koo, Biomaterials 101 (2016) 272–284.
[75] H. Sun, N. Gao, K. Dong, J. Ren, X. Qu, ACS Nano 8 (2014) 6202–6210.
[76] G. Hwang, A.J. Paula, E.E. Hunter, Y. Liu, A. Babeer, B. Karabucak, K. Stebe, V. Kumar, E. Steager, H. Koo, Sci. Rob. 4 (2019) eaaw2388.
[77] K. Quan, Z. Zhang, H. Chen, X. Ren, Y. Ren, B.W. Peterson, H.C. van der Mei, H.J. Busscher,Small 15 (2019), 1902313.
[78] S. Tian, L. Su, Y. Liu, J. Cao, G. Yang, Y. Ren, F. Huang, J. Liu, Y. An, H.C. van der Mei, H.J. Busscher, L. Shi, Sci. Adv. (2020), in press.